Acta Cryst E CRYSTALLOGRAPHIC COMMUNICATIONS

ISSN 2056-9890

Crystal structure, Hirshfeld surface analysis and DFT study of (2*Z*)-2-(4-fluorobenzylidene)-4-(prop-2-yn-1-yl)-3,4-dihydro-2*H*-1,4-benzothiazin-3-one

Brahim Hni,[a]* Nada Kheira Sebbar,[b,a] Tuncer Hökelek,[c] Younes Ouzidan,[d] Ahmed Moussaif,[e] Joel T. Mague[f] and El Mokhtar Essassi[a,g]

[a]Laboratoire de Chimie Organique Hétérocyclique URAC 21, Pôle de Compétence Pharmacochimie, Av. Ibn Battouta, BP 1014, Faculté des Sciences, Université Mohammed V, Rabat, Morocco, [b]Laboratoire de Chimie Bioorganique Appliquée, Faculté des Sciences, Université Ibn Zohr, Agadir, Morocco, [c]Department of Physics, Hacettepe University, 06800 Beytepe, Ankara, Turkey, [d]Laboratoire de Chimie Organique Appliquée, Université Sidi Mohamed Ben Abdallah, Faculté des Sciences et Techniques, Route d'immouzzer, BP 2202, Fez, Morocco, [e]National Center of Energy Sciences and Nuclear Techniques, Rabat, Morocco, [f]Department of Chemistry, Tulane University, New Orleans, LA 70118, USA, and [g]Moroccan Foundation for Advanced Science, Innovation and Research (MASCIR), Rabat, Morocco. *Correspondence e-mail: brahimhni2018@gmail.com

Received 31 January 2019
Accepted 14 February 2019

Edited by A. J. Lough, University of Toronto, Canada

Keywords: crystal structure; dihydrobenzothiazine; hydrogen bond; DFT; Hirshfeld surface.

CCDC reference: 1897371

Supporting information: this article has supporting information at journals.iucr.org/e

The title compound, $C_{18}H_{12}FNOS$, is built up from a 4-fluorobenzylidene moiety and a dihydrobenzothiazine unit with a propynyl substituent, with the heterocyclic portion of the dihydrobenzothiazine unit adopting a shallow boat conformation with the propynyl substituent nearly perpendicular to it. The two benzene rings are oriented at a dihedral angle of 43.02 (6)°. In the crystal, C—$H_{Flurphen}\cdots F_{Flurphen}$ (Flurphen = fluorophenyl) hydrogen bonds link the molecules into inversion dimers, enclosing $R_2^2(8)$ ring motifs, with the dimers forming oblique stacks along the *a*-axis direction. Hirshfeld surface analysis of the crystal structure indicates that the most important contributions to the crystal packing are from H···H (33.9%), H···C/C···H (26.7%), H···F/F···H (10.9%) and C···C (10.6%) interactions. Hydrogen bonding and van der Waals interactions are the dominant interactions in the crystal packing. Density functional theory (DFT) optimized structures at the B3LYP/6–311 G(d,p) level are compared with the experimentally determined molecular structure in the solid state. The HOMO–LUMO behaviour was elucidated to determine the energy gap.

1. Chemical context

1,4-Benzothiazine derivatives represent one of the most important classes of organic molecules and have been studied extensively for their biological activities (Ellouz *et al.*, 2017*a*; Sebbar *et al.*, 2016*a*) and therapeutic applications such as analgesic (Wammack *et al.*, 2002), anti-viral (Malagu *et al.*, 1998; Rathore & Kumar, 2006) and anti-oxidant activities (Zia-ur-Rehman *et al.*, 2009). Slight changes in the substitution pattern in the benzothiazine nucleus can cause a distinguishable difference in their biological properties (Niewiadomy *et al.*, 2011; Armenise *et al.*, 2012). Recent research has been focused on existing molecules and their modifications in order to reduce their side effects and to explore their other pharmacological and biological effects (Ellouz *et al.*, 2017*b*; Sebbar *et al.*, 2016*b*; Gautam *et al.*, 2012). As a continuation of our research into the development of N-substituted 1,4-benzothiazine derivatives and the evaluation of their potential pharmacological activities, we have studied the condensation reaction of propargyl bromide with (*Z*)-2-(4-fluorobenzyl-

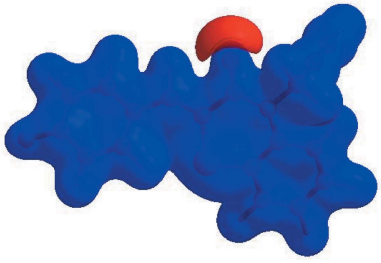

idene)-2*H*-1,4-benzothiazin-3(4*H*)-one under phase-transfer catalysis conditions using tetra-*n*-butylammonium bromide (TBAB) as catalyst and potassium carbonate as base, leading to the title compound namely (2*Z*)-2-(4-fluorobenzylidene)-4-(prop-2-yn-1-yl)-3,4-dihydro-2*H*-1,4-benzothiazin-3-one in good yield (Sebbar *et al.*, 2017*a*, Ellouz *et al.*, 2018), and we report herein its synthesis, the molecular and crystal structures, along with the Hirshfeld surface analysis and density functional theory (DFT) computational calculations carried out at the B3LYP/6–311 G(d,p) level.

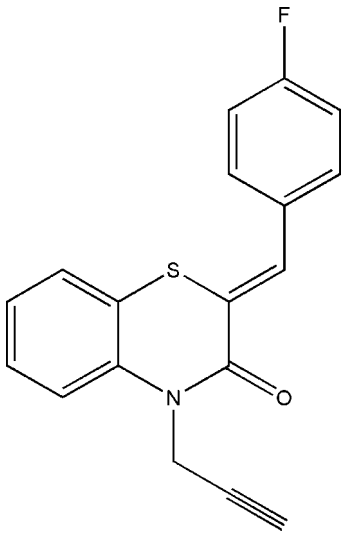

2. Structural commentary

The title compound, (I), is built up from a 4-fluorophenylmethylidene moiety and a dihydrobenzothiazine unit with a propynyl substituent (Fig. 1). The benzene (*A*; C1–C6), ring is oriented at a dihedral angle of 43.02 (6)° with respect to the 4-fluorophenyl ring (*C*; C13–C18). The propynyl substituent is nearly perpendicular to the plane defined by C1, C6, C7 and C8, as shown by the C6—N1—C9—C10 torsion angle of 81.3 (2)°. A puckering analysis of the heterocyclic ring (*B*; S1/N1/C1/C6–C8) of the dihydrobenzothiazine unit shows that it adopts a shallow boat conformation with puckering parameters Q_T = 0.3759 (14) Å, q_2 = 0.3639 (15) Å, q_3 = −0.0938 (17) Å, φ = 173.6 (3)° and θ = 104.5 (3)°. In the heterocyclic ring *B*, the C1—S1—C8 [101.73 (8)°], S1—C8—C7 [119.93 (12)°], C8—C7—N1 [119.23 (14)°], C7—N1—C6 [125.59 (14)°] and C6—C1—S1 [122.07 (13)°] bond angles are enlarged, while the N1—C6—C1 [120.91 (15)°] bond angle is narrowed when compared with the corresponding values in the closely related compounds 4-methyl-3,4-dihydro-2*H*-1,4-benzothiazin-3-one, (II) (Ellouz *et al.*, 2017*b*), 4-[(3-phenyl-4,5-dihydroisoxazol-5-yl) methyl]-2*H*-benzo[*b*][1,4]thiazin-3(4*H*)-one, (III) (Sebbar *et al.*, 2016*a*) and (*Z*)-2-(2-chlorobenzylidene)-4-(prop-2-ynyl)-2*H*-1,4-benzothiazin-3(4*H*)-one, (IV), (Sebbar *et al.*, 2017*a*).

Table 1
Hydrogen-bond geometry (Å, °).

D—H···*A*	*D*—H	H···*A*	*D*···*A*	*D*—H···*A*
C15—H15···F1^{ii}	0.98 (2)	2.60 (2)	3.306 (2)	128.5 (17)

Symmetry code: (ii) $-x-1, -y, -z$.

3. Supramolecular features

In the crystal, C—$H_{Flurphen}$···$F_{Flurphen}$ (Flurphen = fluorophenyl) hydrogen bonds (Table 1) link the molecules into inversion dimers enclosing $R_2^2(8)$ ring motifs, with the dimers forming oblique stacks along the *a*-axis direction (Figs. 2 and 3).

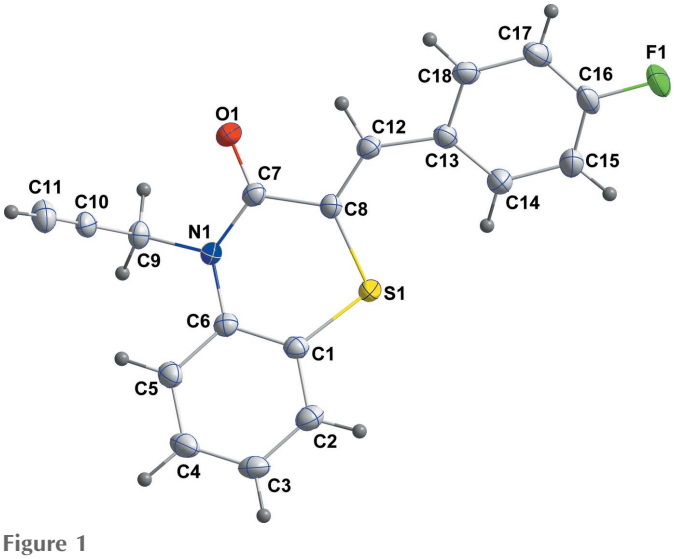

Figure 1
The molecular structure of the title compound with the atom-numbering scheme. Displacement ellipsoids are drawn at the 50% probability level.

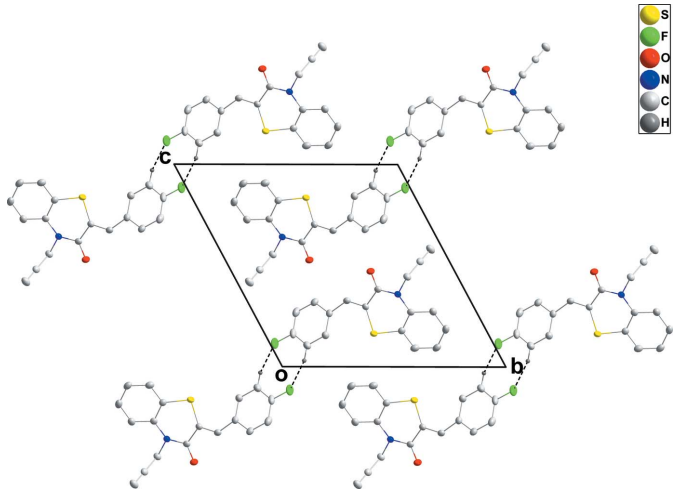

Figure 2
A partial packing diagram viewed along the *a*-axis direction. The intermolecular C—$H_{Flurphen}$···$F_{Flurphen}$ (Flurphen = fluorophenyl) hydrogen bonds are shown as dashed lines.

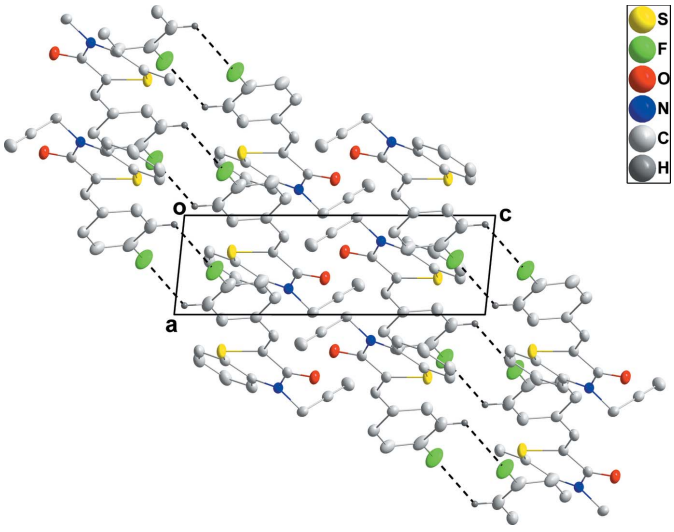

Figure 3
A partial packing diagram viewed along the *b*-axis direction. The intermolecular $C-H_{Flurphen}\cdots F_{Flurphen}$ (Flurphen = fluorophenyl) hydrogen bonds are shown as dashed lines.

4. Hirshfeld surface analysis

In order to visualize the intermolecular interactions in the crystal of the title compound, a Hirshfeld surface (HS) analysis (Hirshfeld, 1977; Spackman & Jayatilaka, 2009) was carried out by using *CrystalExplorer17.5* (Turner *et al.*, 2017). In the HS plotted over d_{norm} (Fig. 4), the white surface indicates contacts with distances equal to the sum of van der Waals radii, and the red and blue colours indicate distances shorter (in close contact) or longer (distinct contact) than the van der Waals radii, respectively (Venkatesan *et al.*, 2016). The bright-red spots indicate their roles as the respective donors and/or acceptors; they also appear as blue and red regions corresponding to positive and negative potentials on the HS mapped over electrostatic potential (Spackman *et al.*, 2008; Jayatilaka *et al.*, 2005) as shown in Fig. 5. The blue regions indicate the positive electrostatic potential (hydrogen-bond donors), while the red regions indicate the negative electrostatic potential (hydrogen-bond acceptors). The shape-index of the HS is a tool to visualize the π–π stacking by the presence of adjacent red and blue triangles; if there are no adjacent red and/or blue triangles, then there are no π– π interactions. Fig. 6 clearly suggest that there are no π– π interactions in (I).

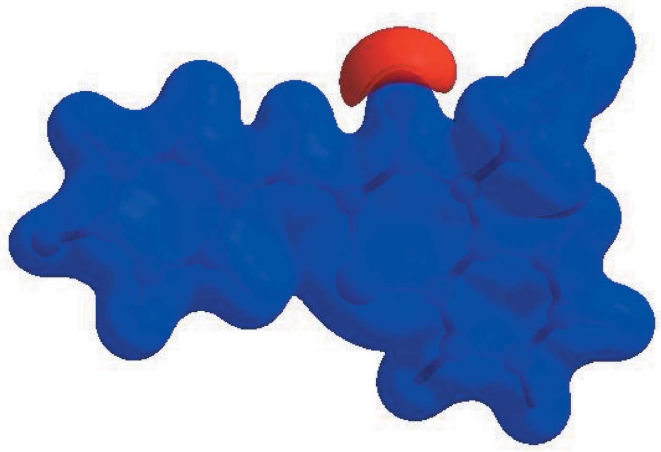

Figure 5
View of the three-dimensional Hirshfeld surface of the title compound plotted over electrostatic potential energy in the range −0.0500 to 0.0500 a.u. using the STO-3 G basis set at the Hartree–Fock level of theory. Hydrogen-bond donors and acceptors are shown as blue and red regions around the atoms corresponding to positive and negative potentials, respectively.

The overall two-dimensional fingerprint plot, Fig. 7*a*, and those delineated into H···H, H···C/C···H, H···F/F···H, C···C, H···O/O···H, H···S/S···H, C···N/N···C, C···S/S···C, C···F/F···C, S···S and H···N/N···H contacts (McKinnon *et al.*, 2007) are illustrated in Fig. 7 *b*–*l*, respectively, together with their relative contributions to the Hirshfeld surface. The most important interaction is H···H contributing 33.9% to the overall crystal packing, which is

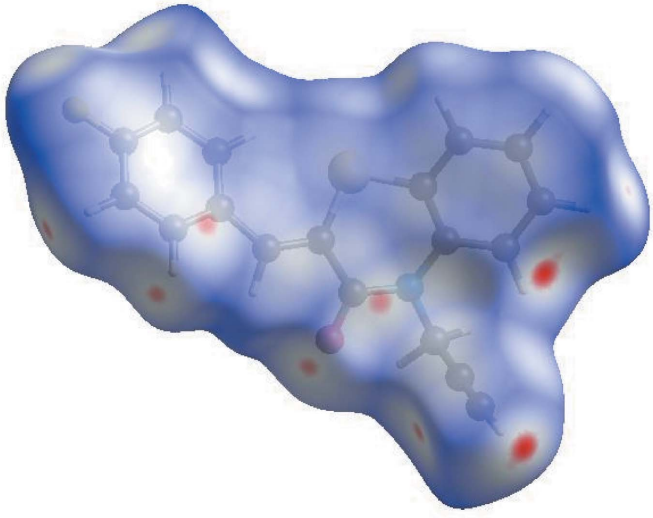

Figure 4
View of the three-dimensional Hirshfeld surface of the title compound plotted over d_{norm} in the range −0.0943 to 1.2826 a.u.

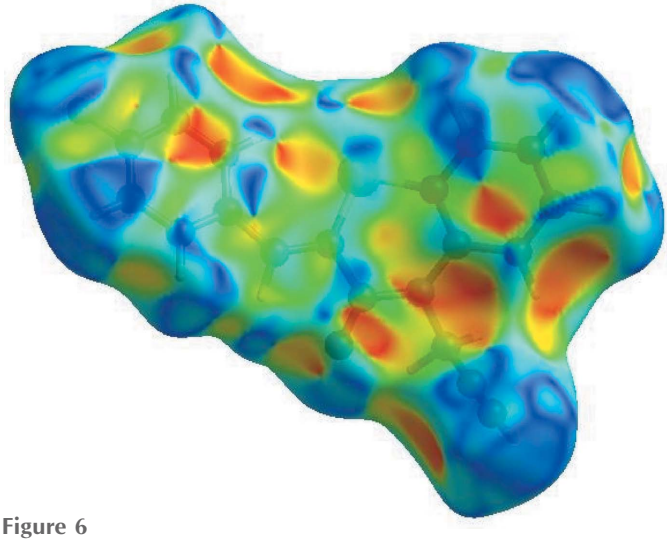

Figure 6
Hirshfeld surface of the title compound plotted over shape-index.

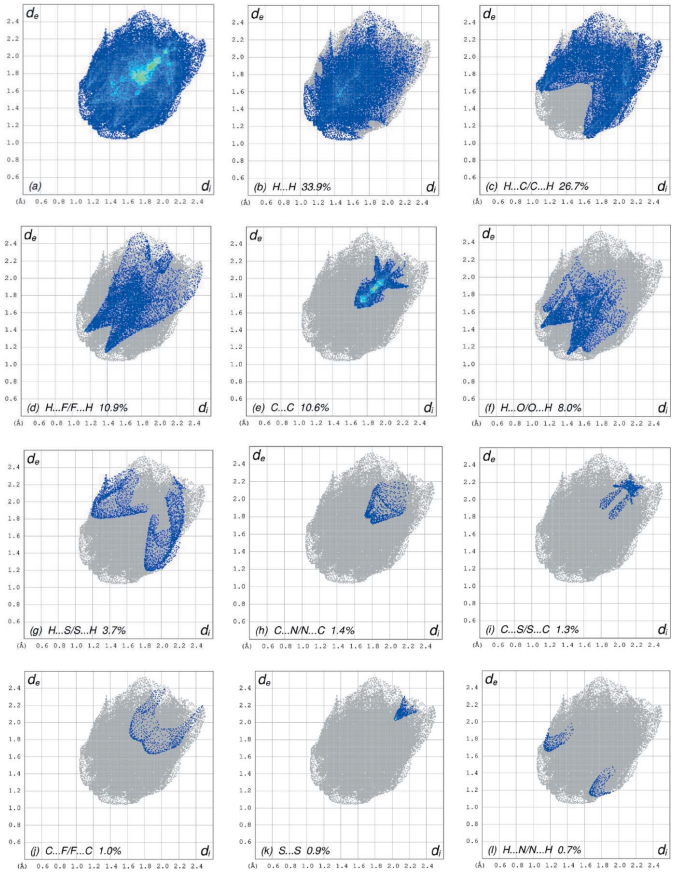

Figure 7
The full two-dimensional fingerprint plots for the title compound, showing (*a*) all interactions, and delineated into (*b*) H···H, (*c*) H···C/C···H, (*d*) H···F/F···H, (*e*) C···C, (*f*) H···O/O···H, (*g*) H···S/S···H, (*h*) C···N/N···C, (*i*) C···S/S···C, (*j*) C···F/F···C, (*k*) S···S and (*l*) H···N/N···H interactions. The d_i and d_e values are the closest internal and external distances (in Å) from given points on the Hirshfeld surface.

reflected in Fig. 7*b* as widely scattered points of high density due to the large hydrogen content of the molecule. In the absence of C—H···π interactions, the pair of scattered wings in the fingerprint plot delineated into H···C/C···H contacts (26.7% contribution to the HS) have a nearly symmetrical distribution of points, Fig. 7*c*, with the thick edges at $d_e + d_i$ ~2.70 Å. The pair of characteristic wings in the fingerprint plot delineated into H···F/F···H contacts (Fig. 7*d*, the 10.9% contribution to the HS) arises from the C—H···F hydrogen bonds (Table 1) as well as from the H···F/F···H contacts (Table 2) and is shown as a pair of spikes with the tips at $d_e + d_i$ = 2.52 Å. The C···C contacts (Fig. 7*e*, 10.6% contribution to the HS) have an arrow-shaped distribution of points with the tip at $d_e = d_i$ ~1.68 Å. The pair of characteristic wings in the fingerprint plot delineated into H···O/O···H contacts (Fig. 7*f*, 8.0% contribution to the HS) have a pair of spikes with the tips at $d_e + d_i$ = 2.54 Å. Finally, the H···S/S···H contacts (Table 2; Fig. 7*g*, 3.7% contribution) are viewed as A pair of wide spikes with the tips at $d_e + d_i$ = 3.02 Å. The Hirshfeld surface representations with the function d_{norm} plotted onto the surface are shown for the H···H, H···C/C···H, H···F/F···H, C···C, H···O/O···H and H···S/S···H interactions in Fig. 8*a–f*, respectively.

Table 2
Selected interatomic distances (Å).

S1···N1	3.0702 (15)	C10···C11^{vii}	3.572 (3)
S1···C14	3.179 (2)	C12···C18^{vii}	3.343 (3)
S1···C2^{i}	3.5158 (19)	C13···C18^{vii}	3.464 (2)
S1···H14	2.51 (3)	C13···C17^{vii}	3.439 (3)
S1···H2^{i}	3.06 (2)	C14···C17^{vii}	3.404 (3)
F1···F1^{ii}	3.051 (2)	C14···C16^{vii}	3.457 (3)
F1···C15^{ii}	3.306 (3)	C15···C16^{vii}	3.495 (3)
F1···H4^{iii}	2.59 (3)	C4···H11^{viii}	2.91 (3)
F1···H15^{ii}	2.60 (2)	C5···H9*B*	2.63 (2)
O1···C10	3.167 (3)	C5···H11^{viii}	2.80 (3)
O1···C18^{iv}	3.388 (2)	C6···H9*B*^{vi}	2.85 (2)
O1···C18^{v}	3.261 (2)	C7···H9*A*^{vi}	2.81 (2)
O1···H12	2.33 (2)	C8···H14	2.97 (2)
O1···H9*A*^{vi}	2.83 (2)	C9···H5	2.48 (3)
O1···H9*A*	2.26 (2)	C10···H5	2.60 (2)
O1···H12^{v}	2.70 (2)	C10···H9*B*^{vi}	2.90 (2)
O1···H18^{iv}	2.60 (2)	C11···H5^{ix}	2.81 (3)
O1···H18^{v}	2.71 (2)	C11···H9*B*^{vi}	2.99 (2)
N1···H9*B*^{vi}	2.85 (2)	C11···H17^{iv}	2.82 (3)
C5···C10	3.216 (2)	H2···H2^{x}	2.57 (4)
C7···C12^{vii}	3.448 (3)	H5···H9*B*	2.17 (3)
C7···C9^{vi}	3.334 (3)	H5···H11^{viii}	2.52 (4)
C9···C10^{vii}	3.504 (2)	H9*A*···H18^{v}	2.50 (3)
C9···C11^{vii}	3.469 (3)	H12···H18	2.32 (3)

Symmetry codes: (i) $-x+1, -y+1, -z$; (ii) $-x-1, -y, -z$; (iii) $x-1, y-1, z$; (iv) $-x, -y+1, -z+1$; (v) $-x+1, -y+1, -z+1$; (vi) $x-1, y, z$; (vii) $x+1, y, z$; (viii) $-x+1, -y+2, -z+1$; (ix) $-x+2, -y+2, -z+1$; (x) $-x, -y+1, -z$.

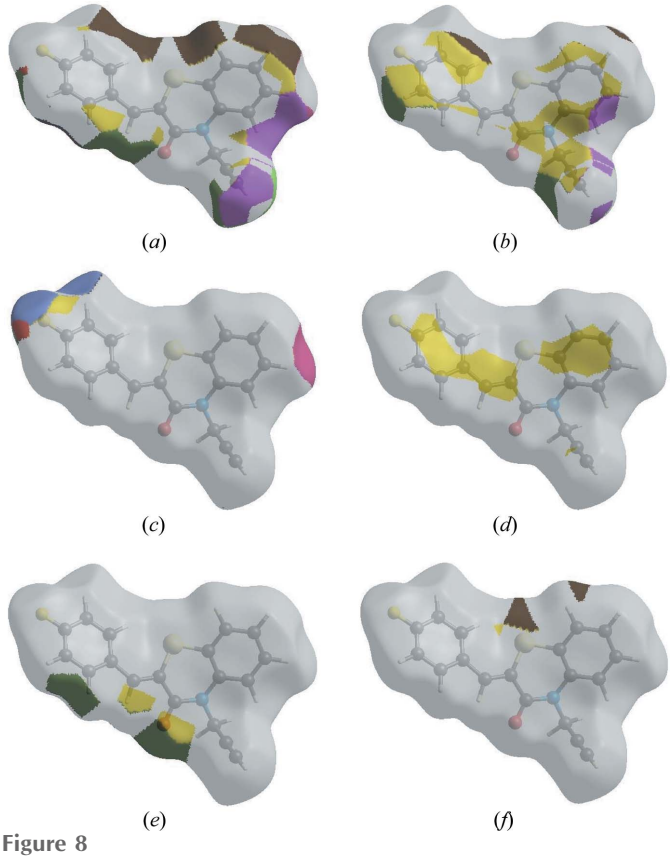

Figure 8
The Hirshfeld surface representations with the function d_{norm} plotted onto the surface for (*a*) H···H, (*b*) H···C/C···H, (*c*) H···F/F···H, (*d*) C···C, (*e*) H···O/O···H and (*f*) H···S/S···H interactions.

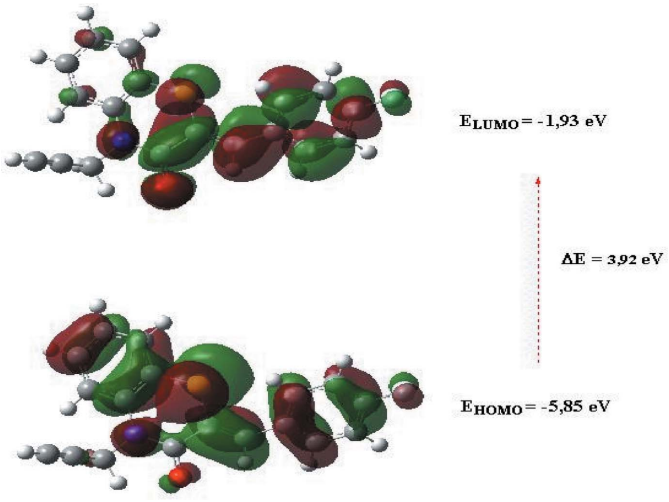

Figure 9
The energy band gap of the title compound.

The Hirshfeld surface analysis confirms the importance of H-atom contacts in establishing the packing. The large number of H···H, H···C/C···H and H···O/O···H interactions suggest that van der Waals interactions and hydrogen bonding play the major roles in the crystal packing (Hathwar *et al.*, 2015).

5. DFT calculations

The optimized structure of the title compound, (I), in the gas phase was generated theoretically *via* density functional theory (DFT) using standard B3LYP functional and 6–311G(d,p) basis-set calculations (Becke, 1993) as implemented in *GAUSSIAN 09* (Frisch *et al.*, 2009). The theoretical and experimental results were in good agreement. The highest-occupied molecular orbital (HOMO), acting as an electron donor, and the lowest-unoccupied molecular orbital (LUMO), acting as an electron acceptor, are very important parameters for quantum chemistry. When the energy gap is small, the molecule is highly polarizable and has high chemical reactivity. The electron transition from the HOMO to the LUMO energy level is shown in Fig. 9. The HOMO and LUMO are localized in the plane extending from the whole (*Z*)-2-(4-fluorobenzylidene)-4-(prop-2-ynyl)-2*H*-1,4-benzothiazin-3(4*H*)-one ring. The energy band gap [$\Delta E = E_{LUMO} - E_{HOMO}$] of the molecule was about 3.92 eV, and the frontier molecular orbital energies, E_{HOMO} and E_{LUMO} were −5.85 and −1.93 eV, respectively.

6. Database survey

Using the search fragment **II** (R_1 = Ph, R_2 = C) in the Cambridge Crystallographic Database (Groom *et al.*, 2016; updated to Nov. 2018), 14 hits were registered with R_1 = Ph and R_2 = CH_2COOH (Sebbar *et al.*, 2016*c*), **IIa** (Sebbar *et al.*, 2016*b*), *n*-octadecyl (Sebbar *et al.*, 2017*b*), **IIb** (Ellouz *et al.*, 2015), *n*-Bu (Sebbar, El Fal *et al.*, 2014), **IIc** (Sebbar *et al.*, 2016*d*), **IId** (Sebbar *et al.*, 2015), $CH_2C{\equiv}CH$ **IIe** (Sebbar, Zerzouf *et al.*, 2014). In addition there are examples with R_1 = 4-ClC_6H_4 and R_2 = CH_2Ph2 (Ellouz *et al.*, 2016) **IIf** and R_1 = 2-ClC_6H_4, R_2 = $CH_2C{\equiv}CH$ (Sebbar *et al.*, 2017*c*). In the majority of these, the heterocyclic ring is quite non-planar with the dihedral angle between the plane defined by the benzene ring plus the nitrogen and sulfur atoms and that defined by nitrogen and sulfur and the other two carbon atoms separating them ranging from ca. 29 (**IIe**) to 36° (**IId**). The other three (**IIa**, **IIc**, **IIf**) have the benzothiazine unit nearly planar with the corresponding dihedral angle of *ca* 3–4°. In the case of **IIa**, the displacement ellipsoid for the sulfur atom shows a considerable elongation perpendicular to the mean plane of the heterocyclic ring, suggesting disorder, and a greater degree of non-planarity but for the other two, there is no obvious source for the near planarity.

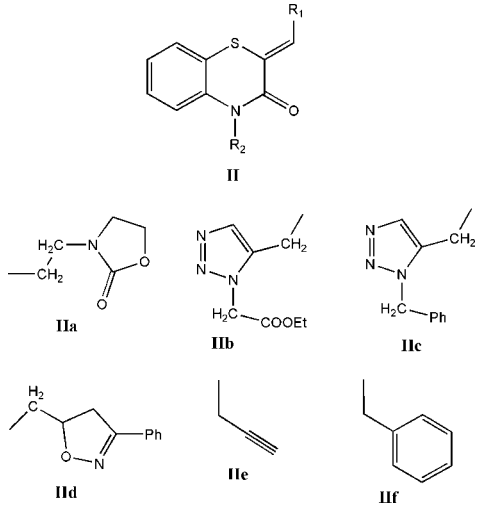

7. Synthesis and crystallization

Propargyl bromide (4 mmol) was added to a mixture of (*Z*)-2-(4-fluorobenzylidene)-2*H*-1,4-benzothiazin-3(4*H*)-one (1.6 mmol), potassium carbonate (4 mmol) and tetra-*n*-butyl ammonium bromide (0.15 mmol) in DMF (20 ml). Stirring was continued at room temperature for 24 h. The salts were removed by filtration and the filtrate was concentrated under reduced pressure. The residue was separated by chromatography on a column of silica gel with ethyl acetate–hexane (2/8) as eluent. The solid product obtained was recrystallized from ethanol to afford colourless crystals (yield: 89%).

8. Refinement

Crystal data, data collection and structure refinement details are summarized in Table 3. Hydrogen atoms were located in a difference-Fourier map and freely refined.

Funding information

The support of NSF–MRI grant No. 1228232 for the purchase of the diffractometer and Tulane University for support of the

Tulane Crystallography Laboratory are gratefully acknowledged. TH is grateful to the Hacettepe University Scientific Research Project Unit (grant No. 013 D04 602 004).

References

Armenise, D., Muraglia, M., Florio, M. A., De Laurentis, N., Rosato, A., Carrieri, A., Corbo, F. & Franchini, C. (2012). *Arch. Pharm. Pharm. Med. Chem.* **345**, 407–416.

Becke, A. D. (1993). *J. Chem. Phys.* **98**, 5648–5652.

Brandenburg, K. & Putz, H. (2012). *DIAMOND*, Crystal Impact GbR, Bonn, Germany.

Bruker (2016). *APEX3*, *SAINT* and *SADABS*. Bruker AXS, Inc., Madison, Wisconsin, USA.

Ellouz, M., Sebbar, N. K., Boulhaoua, M., Essassi, E. M. & Mague, J. T. (2017*a*). *IUCrData*, **2**, x170646.

Ellouz, M., Sebbar, N. K., Essassi, E. M., Ouzidan, Y. & Mague, J. T. (2015). *Acta Cryst.* E**71**, o1022–o1023.

Ellouz, M., Sebbar, N. K., Essassi, E. M., Ouzidan, Y., Mague, J. T. & Zouihri, H. (2016). *IUCrData*, **1**, x160764.

Ellouz, M., Sebbar, N. K., Fichtali, I., Ouzidan, Y., Mennane, Z., Charof, R., Mague, J. T., Urrutigoïty, M. & Essassi, E. M. (2018). *Chem. Cent. J.* **12**, 123.

Ellouz, M., Sebbar, N. K., Ouzidan, Y., Essassi, E. M. & Mague, J. T. (2017*b*). *IUCrData*, **2**, x170097.

Frisch, M. J., Trucks, G. W., Schlegel, H. B., Scuseria, G. E., Robb, M. A., Cheeseman, J. R., *et al.* (2009). *GAUSSIAN09*. Gaussian Inc., Wallingford, CT, USA.

Gautam, N., Ajmera, N., Gupta, S. & Gautam, D. C. (2012). *Eur. J. Chem.* **3**, 106–111.

Groom, C. R., Bruno, I. J., Lightfoot, M. P. & Ward, S. C. (2016). *Acta Cryst.* B**72**, 171–179.

Hathwar, V. R., Sist, M., Jørgensen, M. R. V., Mamakhel, A. H., Wang, X., Hoffmann, C. M., Sugimoto, K., Overgaard, J. & Iversen, B. B. (2015). *IUCrJ*, **2**, 563–574.

Hirshfeld, H. L. (1977). *Theor. Chim. Acta*, **44**, 129–138.

Jayatilaka, D., Grimwood, D. J., Lee, A., Lemay, A., Russel, A. J., Taylor, C., Wolff, S. K., Cassam-Chenai, P. & Whitton, A. (2005). *TONTO – A System for Computational Chemistry. Available at: http://hirshfeldsurface.net/*

Krause, L., Herbst-Irmer, R., Sheldrick, G. M. & Stalke, D. (2015). *J. Appl. Cryst.* **48**, 3–10.

Malagu, K., Boustie, J., David, M., Sauleau, J., Amoros, M., Girre, R. L. & Sauleau, A. (1998). *Pharm. Pharmacol. Commun.* **4**, 57–60.

McKinnon, J. J., Jayatilaka, D. & Spackman, M. A. (2007). *Chem. Commun.* pp. 3814–3816.

Niewiadomy, A., Matysiak, J. & Karpińska, M. M. (2011). *Arch. Pharm. Pharm. Med. Chem.* **344**, 224–230.

Rathore, B. S. & Kumar, M. (2006). *Bioorg. Med. Chem.* **14**, 5678–5682.

Sebbar, N. K., El Fal, M., Essassi, E. M., Saadi, M. & El Ammari, L. (2014). *Acta Cryst.* E**70**, o686.

Sebbar, N. K., Ellouz, M., Boulhaoua, M., Ouzidan, Y., Essassi, E. M. & Mague, J. T. (2016*d*). *IUCrData*, **1**, x161823.

Sebbar, N. K., Ellouz, M., Essassi, E. M., Saadi, M. & El Ammari, L. (2015). *Acta Cryst.* E**71**, o423–o424.

Sebbar, N. K., Ellouz, M., Essassi, E. M., Saadi, M. & El Ammari, L. (2016*a*). *IUCr Data* **1**, x161012.

Sebbar, N. K., Ellouz, M., Lahmidi, S., Hlimi, F., Essassi, E. & Mague, J. T. (2017*b*). *IUCrData*, **2**, x170695.

Table 3
Experimental details.

Crystal data	
Chemical formula	$C_{18}H_{12}FNOS$
M_r	309.35
Crystal system, space group	Triclinic, $P\overline{1}$
Temperature (K)	150
a, b, c (Å)	4.0602 (2), 13.8983 (5), 14.2620 (5)
α, β, γ (°)	117.809 (2), 93.155 (2), 94.416 (2)
V (Å^3)	705.96 (5)
Z	2
Radiation type	Cu $K\alpha$
μ (mm^{-1})	2.15
Crystal size (mm)	0.45 × 0.21 × 0.01
Data collection	
Diffractometer	Bruker D8 VENTURE PHOTON 100 CMOS
Absorption correction	Numerical (*SADABS*; Krause *et al.*, 2015)
T_{min}, T_{max}	0.69, 0.97
No. of measured, independent and observed [$I > 2\sigma(I)$] reflections	5323, 2595, 2256
R_{int}	0.026
(sin $\theta/\lambda)_{max}$ (Å^{-1})	0.618
Refinement	
$R[F^2 > 2\sigma(F^2)]$, $wR(F^2)$, S	0.036, 0.092, 1.04
No. of reflections	2595
No. of parameters	247
H-atom treatment	All H-atom parameters refined
$\Delta\rho_{max}$, $\Delta\rho_{min}$ (e Å^{-3})	0.23, −0.31

Computer programs: *APEX3* and *SAINT* (Bruker, 2016), *SHELXT* (Sheldrick, 2015*a*), *SHELXL2018* (Sheldrick, 2015*b*), *DIAMOND* (Brandenburg & Putz, 2012) and *SHELXTL* (Sheldrick, 2008).

Sebbar, N. K., Ellouz, M., Mague, J. T., Ouzidan, Y., Essassi, E. M. & Zouihri, H. (2016*c*). *IUCrData*, **1**, x160863.

Sebbar, N. K., Ellouz, M., Ouzidan, Y., Kaur, M., Essassi, E. M. & Jasinski, J. P. (2017*a*). *IUCrData*, **2**, x170889.

Sebbar, N. K., Ellouz, M., Ouzidan, Y., Kaur, M., Essassi, E. M. & Jasinski, J. P. (2017*c*). *IUCrData*, **2**, x170889.

Sebbar, N. K., Mekhzoum, M. E. M., Essassi, E. M., Zerzouf, A., Talbaoui, A., Bakri, Y., Saadi, M. & Ammari, L. E. (2016*b*). *Res. Chem. Intermed.* **42**, 6845–6862.

Sebbar, N. K., Zerzouf, A., Essassi, E. M., Saadi, M. & El Ammari, L. (2014). *Acta Cryst.* E**70**, o614.

Sheldrick, G. M. (2008). *Acta Cryst.* A**64**, 112–122.

Sheldrick, G. M. (2015*a*). *Acta Cryst.* A**71**, 3–8.

Sheldrick, G. M. (2015*b*). *Acta Cryst.* C**71**, 3–8.

Spackman, M. A. & Jayatilaka, D. (2009). *CrystEngComm*, **11**, 19–32.

Spackman, M. A., McKinnon, J. J. & Jayatilaka, D. (2008). *CrystEngComm*, **10**, 377–388.

Turner, M. J., McKinnon, J. J., Wolff, S. K., Grimwood, D. J., Spackman, P. R., Jayatilaka, D. & Spackman, M. A. (2017). *CrystalExplorer17*. The University of Western Australia.

Venkatesan, P., Thamotharan, S., Ilangovan, A., Liang, H. & Sundius, T. (2016). *Spectrochim. Acta A Mol. Biomol. Spectrosc.* **153**, 625–636.

Wammack, R., Remzi, M., Seitz, C., Djavan, B. & Marberger, M. (2002). *Eur. Urol.* **41**, 596–601.

Zia-ur-Rehman, M., Choudary, J. A., Elsegood, M. R. J., Siddiqui, H. L. & Khan, K. M. (2009). *Eur. J. Med. Chem.* **44**, 1311–1316.

supporting information

Acta Cryst. (2019). E**75**, 372-377 [https://doi.org/10.1107/S2056989019002354]

Crystal structure, Hirshfeld surface analysis and DFT study of (2*Z*)-2-(4-fluorobenzylidene)-4-(prop-2-yn-1-yl)-3,4-dihydro-2*H*-1,4-benzothiazin-3-one

Brahim Hni, Nada Kheira Sebbar, Tuncer Hökelek, Younes Ouzidan, Ahmed Moussaif, Joel T. Mague and El Mokhtar Essassi

Computing details

Data collection: *APEX3* (Bruker, 2016); cell refinement: *SAINT* (Bruker, 2016); data reduction: *SAINT* (Bruker, 2016); program(s) used to solve structure: *SHELXT* (Sheldrick, 2015*a*); program(s) used to refine structure: *SHELXL2018* (Sheldrick, 2015*b*); molecular graphics: *DIAMOND* (Brandenburg & Putz, 2012); software used to prepare material for publication: *SHELXTL* (Sheldrick, 2008).

(2*Z*)-2-(4-Fluorobenzylidene)-4-(prop-2-yn-1-yl)-3,4-dihydro-2*H*-1,4-benzothiazin-3-one

Crystal data

$C_{18}H_{12}FNOS$
$M_r = 309.35$
Triclinic, $P\overline{1}$
$a = 4.0602$ (2) Å
$b = 13.8983$ (5) Å
$c = 14.2620$ (5) Å
$\alpha = 117.809$ (2)°
$\beta = 93.155$ (2)°
$\gamma = 94.416$ (2)°
$V = 705.96$ (5) Å^3
$Z = 2$
$F(000) = 320$
$D_x = 1.455$ Mg m^{-3}
Cu $K\alpha$ radiation, $\lambda = 1.54178$ Å
Cell parameters from 4191 reflections
$\theta = 3.6$–72.3°
$\mu = 2.15$ mm^{-1}
$T = 150$ K
Plate, light yellow
0.45 × 0.21 × 0.01 mm

Data collection

Bruker D8 VENTURE PHOTON 100 CMOS diffractometer
Radiation source: INCOATEC IμS micro-focus source
Mirror monochromator
Detector resolution: 10.4167 pixels mm^{-1}
ω scans
Absorption correction: numerical (*SADABS*; Krause *et al.*, 2015)
$T_{min} = 0.69$, $T_{max} = 0.97$
5323 measured reflections
2595 independent reflections
2256 reflections with $I > 2\sigma(I)$
$R_{int} = 0.026$
$\theta_{max} = 72.2°$, $\theta_{min} = 3.6°$
$h = -4\rightarrow4$
$k = -17\rightarrow15$
$l = -15\rightarrow17$

Refinement

Refinement on F^2
Least-squares matrix: full
$R[F^2 > 2\sigma(F^2)] = 0.036$
$wR(F^2) = 0.092$
$S = 1.04$
2595 reflections
247 parameters
0 restraints
Primary atom site location: structure-invariant direct methods
Secondary atom site location: difference Fourier map

Hydrogen site location: difference Fourier map
All H-atom parameters refined
$w = 1/[\sigma^2(F_o^2) + (0.047P)^2 + 0.2564P]$
where $P = (F_o^2 + 2F_c^2)/3$

$(\Delta/\sigma)_{max} < 0.001$
$\Delta\rho_{max} = 0.23$ e Å^{-3}
$\Delta\rho_{min} = -0.31$ e Å^{-3}

Special details

Geometry. All esds (except the esd in the dihedral angle between two l.s. planes) are estimated using the full covariance matrix. The cell esds are taken into account individually in the estimation of esds in distances, angles and torsion angles; correlations between esds in cell parameters are only used when they are defined by crystal symmetry. An approximate (isotropic) treatment of cell esds is used for estimating esds involving l.s. planes.

Refinement. Refinement of F^2 against ALL reflections. The weighted R-factor wR and goodness of fit S are based on F^2, conventional R-factors R are based on F, with F set to zero for negative F^2. The threshold expression of $F^2 > 2\text{sigma}(F^2)$ is used only for calculating R-factors(gt) etc. and is not relevant to the choice of reflections for refinement. R-factors based on F^2 are statistically about twice as large as those based on F, and R- factors based on ALL data will be even larger.

Fractional atomic coordinates and isotropic or equivalent isotropic displacement parameters (Å^2)

	x	*y*	*z*	U_{iso}*/U_{eq}
S1	0.36900 (11)	0.48920 (3)	0.16432 (3)	0.02650 (14)
F1	−0.4439 (4)	0.02242 (10)	0.11539 (11)	0.0500 (4)
O1	0.6330 (3)	0.62345 (10)	0.47251 (9)	0.0274 (3)
N1	0.7395 (3)	0.69008 (11)	0.35897 (11)	0.0196 (3)
C1	0.4638 (4)	0.62082 (14)	0.17880 (13)	0.0216 (3)
C2	0.3701 (5)	0.63770 (16)	0.09280 (14)	0.0280 (4)
H2	0.244 (6)	0.5760 (19)	0.0305 (18)	0.040 (6)*
C3	0.4589 (5)	0.73747 (16)	0.09560 (15)	0.0302 (4)
H3	0.400 (5)	0.7482 (18)	0.0363 (18)	0.035 (6)*
C4	0.6386 (5)	0.82155 (16)	0.18618 (16)	0.0309 (4)
H4	0.717 (5)	0.8918 (19)	0.1894 (17)	0.037 (6)*
C5	0.7262 (4)	0.80684 (15)	0.27349 (14)	0.0253 (4)
H5	0.838 (6)	0.8665 (19)	0.3380 (18)	0.034 (6)*
C6	0.6440 (4)	0.70567 (14)	0.27073 (13)	0.0200 (3)
C7	0.5847 (4)	0.61287 (13)	0.38287 (13)	0.0201 (3)
C8	0.3693 (4)	0.51633 (13)	0.29720 (13)	0.0200 (3)
C9	0.9780 (4)	0.77412 (14)	0.44531 (14)	0.0226 (4)
H9A	1.078 (5)	0.7384 (17)	0.4841 (16)	0.027 (5)*
H9B	1.157 (5)	0.7991 (17)	0.4139 (16)	0.029 (5)*
C10	0.8244 (4)	0.86876 (14)	0.52130 (13)	0.0232 (4)
C11	0.7008 (5)	0.94494 (16)	0.58223 (16)	0.0323 (4)
H11	0.598 (7)	1.005 (2)	0.627 (2)	0.058 (8)*
C12	0.2140 (4)	0.44701 (14)	0.32673 (13)	0.0221 (4)
H12	0.239 (5)	0.4694 (17)	0.4023 (17)	0.027 (5)*
C13	0.0273 (4)	0.33862 (14)	0.26424 (13)	0.0224 (4)
C14	0.0509 (5)	0.26864 (15)	0.15586 (14)	0.0273 (4)
H14	0.190 (5)	0.2934 (18)	0.1155 (17)	0.033 (6)*
C15	−0.1081 (5)	0.16234 (16)	0.10546 (16)	0.0317 (4)
H15	−0.091 (6)	0.1127 (19)	0.0299 (19)	0.041 (6)*
C16	−0.2926 (5)	0.12750 (16)	0.16410 (17)	0.0337 (4)
C17	−0.3307 (5)	0.19315 (17)	0.26970 (16)	0.0334 (4)

H17	−0.461 (6)	0.166 (2)	0.3075 (19)	0.046 (7)*
C18	−0.1680 (4)	0.29876 (15)	0.31937 (15)	0.0258 (4)
H18	−0.184 (5)	0.3440 (17)	0.3957 (18)	0.029 (5)*

Atomic displacement parameters (Å²)

	U^{11}	U^{22}	U^{33}	U^{12}	U^{13}	U^{23}
S1	0.0385 (3)	0.0213 (2)	0.0162 (2)	−0.00484 (17)	0.00200 (16)	0.00729 (18)
F1	0.0686 (9)	0.0280 (6)	0.0495 (8)	−0.0221 (6)	−0.0186 (6)	0.0217 (6)
O1	0.0346 (7)	0.0275 (7)	0.0186 (6)	−0.0014 (5)	−0.0013 (5)	0.0108 (5)
N1	0.0214 (7)	0.0177 (7)	0.0176 (7)	0.0015 (5)	0.0016 (5)	0.0067 (6)
C1	0.0221 (8)	0.0235 (9)	0.0208 (8)	0.0027 (6)	0.0047 (6)	0.0114 (7)
C2	0.0297 (10)	0.0330 (10)	0.0214 (9)	0.0033 (7)	0.0040 (7)	0.0129 (8)
C3	0.0378 (11)	0.0351 (11)	0.0255 (9)	0.0094 (8)	0.0076 (7)	0.0197 (9)
C4	0.0426 (11)	0.0257 (10)	0.0311 (10)	0.0083 (8)	0.0130 (8)	0.0173 (9)
C5	0.0291 (9)	0.0214 (9)	0.0247 (9)	0.0035 (7)	0.0070 (7)	0.0097 (8)
C6	0.0190 (8)	0.0212 (8)	0.0195 (8)	0.0044 (6)	0.0055 (6)	0.0087 (7)
C7	0.0214 (8)	0.0202 (8)	0.0182 (8)	0.0054 (6)	0.0032 (6)	0.0080 (7)
C8	0.0220 (8)	0.0178 (8)	0.0188 (8)	0.0030 (6)	0.0025 (6)	0.0073 (7)
C9	0.0198 (8)	0.0208 (8)	0.0229 (8)	−0.0001 (6)	−0.0004 (6)	0.0075 (7)
C10	0.0225 (8)	0.0215 (9)	0.0227 (8)	−0.0046 (6)	−0.0010 (6)	0.0095 (7)
C11	0.0336 (11)	0.0231 (10)	0.0321 (10)	−0.0004 (8)	0.0083 (8)	0.0064 (9)
C12	0.0259 (9)	0.0224 (9)	0.0182 (8)	0.0044 (6)	0.0044 (6)	0.0092 (7)
C13	0.0229 (8)	0.0214 (9)	0.0248 (9)	0.0011 (6)	−0.0006 (6)	0.0131 (7)
C14	0.0338 (10)	0.0230 (9)	0.0248 (9)	0.0007 (7)	0.0035 (7)	0.0115 (8)
C15	0.0413 (11)	0.0219 (9)	0.0271 (10)	−0.0005 (8)	−0.0038 (8)	0.0088 (8)
C16	0.0401 (11)	0.0216 (9)	0.0393 (11)	−0.0087 (8)	−0.0132 (8)	0.0178 (8)
C17	0.0338 (10)	0.0346 (11)	0.0381 (11)	−0.0079 (8)	−0.0064 (8)	0.0253 (10)
C18	0.0273 (9)	0.0293 (10)	0.0252 (9)	0.0007 (7)	−0.0013 (7)	0.0173 (8)

Geometric parameters (Å, º)

S1—C8	1.7511 (17)	C8—C12	1.348 (2)
S1—C1	1.7515 (17)	C9—C10	1.471 (2)
F1—C16	1.364 (2)	C9—H9A	0.99 (2)
O1—C7	1.219 (2)	C9—H9B	0.99 (2)
N1—C7	1.387 (2)	C10—C11	1.183 (3)
N1—C6	1.412 (2)	C11—H11	0.93 (3)
N1—C9	1.473 (2)	C12—C13	1.461 (2)
C1—C2	1.391 (2)	C12—H12	0.97 (2)
C1—C6	1.401 (2)	C13—C18	1.400 (2)
C2—C3	1.387 (3)	C13—C14	1.404 (2)
C2—H2	0.98 (2)	C14—C15	1.388 (3)
C3—C4	1.387 (3)	C14—H14	0.98 (2)
C3—H3	0.95 (2)	C15—C16	1.373 (3)
C4—C5	1.385 (3)	C15—H15	0.98 (2)
C4—H4	0.98 (2)	C16—C17	1.375 (3)
C5—C6	1.402 (2)	C17—C18	1.386 (3)

C5—H5	0.96 (2)	C17—H17	0.95 (2)
C7—C8	1.493 (2)	C18—H18	0.98 (2)
S1···N1	3.0702 (15)	C10···C11^{vii}	3.572 (3)
S1···C14	3.179 (2)	C12···C18^{vii}	3.343 (3)
S1···C2^{i}	3.5158 (19)	C13···C18^{vii}	3.464 (2)
S1···H14	2.51 (3)	C13···C17^{vii}	3.439 (3)
S1···H2^{i}	3.06 (2)	C14···C17^{vii}	3.404 (3)
F1···F1^{ii}	3.051 (2)	C14···C16^{vii}	3.457 (3)
F1···C15^{ii}	3.306 (3)	C15···C16^{vii}	3.495 (3)
F1···H4^{iii}	2.59 (3)	C4···H11^{viii}	2.91 (3)
F1···H15^{ii}	2.60 (2)	C5···H9B	2.63 (2)
O1···C10	3.167 (3)	C5···H11^{viii}	2.80 (3)
O1···C18^{iv}	3.388 (2)	C6···H9B^{vi}	2.85 (2)
O1···C18^{v}	3.261 (2)	C7···H9A^{vi}	2.81 (2)
O1···H12	2.33 (2)	C8···H14	2.97 (2)
O1···H9A^{vi}	2.83 (2)	C9···H5	2.48 (3)
O1···H9A	2.26 (2)	C10···H5	2.60 (2)
O1···H12^{v}	2.70 (2)	C10···H9B^{vi}	2.90 (2)
O1···H18^{iv}	2.60 (2)	C11···H5^{ix}	2.81 (3)
O1···H18^{v}	2.71 (2)	C11···H9B^{vi}	2.99 (2)
N1···H9B^{vi}	2.85 (2)	C11···H17^{iv}	2.82 (3)
C5···C10	3.216 (2)	H2···H2^{x}	2.57 (4)
C7···C12^{vii}	3.448 (3)	H5···H9B	2.17 (3)
C7···C9^{vi}	3.334 (3)	H5···H11^{viii}	2.52 (4)
C9···C10^{vii}	3.504 (2)	H9A···H18^{v}	2.50 (3)
C9···C11^{vii}	3.469 (3)	H12···H18	2.32 (3)
C8—S1—C1	101.73 (8)	C10—C9—H9A	108.6 (12)
C7—N1—C6	125.59 (14)	N1—C9—H9A	106.8 (12)
C7—N1—C9	114.59 (13)	C10—C9—H9B	109.9 (12)
C6—N1—C9	118.68 (14)	N1—C9—H9B	109.3 (12)
C2—C1—C6	120.19 (16)	H9A—C9—H9B	108.7 (17)
C2—C1—S1	117.64 (14)	C11—C10—C9	179.8 (2)
C6—C1—S1	122.07 (13)	C10—C11—H11	177.1 (17)
C3—C2—C1	120.78 (17)	C8—C12—C13	131.55 (16)
C3—C2—H2	122.1 (14)	C8—C12—H12	115.9 (12)
C1—C2—H2	117.1 (14)	C13—C12—H12	112.4 (12)
C4—C3—C2	119.25 (17)	C18—C13—C14	117.96 (16)
C4—C3—H3	120.1 (14)	C18—C13—C12	116.92 (16)
C2—C3—H3	120.7 (14)	C14—C13—C12	124.90 (16)
C5—C4—C3	120.61 (17)	C15—C14—C13	121.06 (17)
C5—C4—H4	117.9 (13)	C15—C14—H14	118.9 (13)
C3—C4—H4	121.4 (13)	C13—C14—H14	119.9 (13)
C4—C5—C6	120.64 (17)	C16—C15—C14	118.26 (18)
C4—C5—H5	120.7 (14)	C16—C15—H15	120.2 (14)
C6—C5—H5	118.6 (14)	C14—C15—H15	121.5 (14)
C1—C6—C5	118.49 (16)	F1—C16—C15	118.42 (19)

C1—C6—N1	120.91 (15)	F1—C16—C17	118.38 (18)
C5—C6—N1	120.60 (15)	C15—C16—C17	123.20 (18)
O1—C7—N1	119.59 (15)	C16—C17—C18	117.97 (18)
O1—C7—C8	121.15 (15)	C16—C17—H17	120.7 (15)
N1—C7—C8	119.23 (14)	C18—C17—H17	121.4 (15)
C12—C8—C7	116.29 (15)	C17—C18—C13	121.53 (18)
C12—C8—S1	123.30 (13)	C17—C18—H18	117.9 (12)
C7—C8—S1	119.93 (12)	C13—C18—H18	120.5 (12)
C10—C9—N1	113.47 (14)		

C8—S1—C1—C2	−157.17 (14)	N1—C7—C8—C12	−177.04 (15)
C8—S1—C1—C6	26.38 (15)	O1—C7—C8—S1	−167.49 (13)
C6—C1—C2—C3	1.4 (3)	N1—C7—C8—S1	10.7 (2)
S1—C1—C2—C3	−175.12 (14)	C1—S1—C8—C12	159.13 (15)
C1—C2—C3—C4	−1.1 (3)	C1—S1—C8—C7	−29.17 (15)
C2—C3—C4—C5	−0.6 (3)	C7—N1—C9—C10	−87.21 (18)
C3—C4—C5—C6	2.0 (3)	C6—N1—C9—C10	81.32 (18)
C2—C1—C6—C5	0.0 (2)	C7—C8—C12—C13	−169.96 (16)
S1—C1—C6—C5	176.34 (13)	S1—C8—C12—C13	2.0 (3)
C2—C1—C6—N1	179.64 (15)	C8—C12—C13—C18	−165.58 (18)
S1—C1—C6—N1	−4.0 (2)	C8—C12—C13—C14	19.9 (3)
C4—C5—C6—C1	−1.7 (3)	C18—C13—C14—C15	−1.5 (3)
C4—C5—C6—N1	178.67 (16)	C12—C13—C14—C15	172.96 (17)
C7—N1—C6—C1	−23.7 (2)	C13—C14—C15—C16	0.7 (3)
C9—N1—C6—C1	169.12 (14)	C14—C15—C16—F1	−178.73 (17)
C7—N1—C6—C5	155.92 (16)	C14—C15—C16—C17	0.8 (3)
C9—N1—C6—C5	−11.2 (2)	F1—C16—C17—C18	178.11 (17)
C6—N1—C7—O1	−162.11 (15)	C15—C16—C17—C18	−1.5 (3)
C9—N1—C7—O1	5.5 (2)	C16—C17—C18—C13	0.6 (3)
C6—N1—C7—C8	19.7 (2)	C14—C13—C18—C17	0.8 (3)
C9—N1—C7—C8	−172.72 (14)	C12—C13—C18—C17	−174.05 (16)
O1—C7—C8—C12	4.8 (2)		

Symmetry codes: (i) −*x*+1, −*y*+1, −*z*; (ii) −*x*−1, −*y*, −*z*; (iii) *x*−1, *y*−1, *z*; (iv) −*x*, −*y*+1, −*z*+1; (v) −*x*+1, −*y*+1, −*z*+1; (vi) *x*−1, *y*, *z*; (vii) *x*+1, *y*, *z*; (viii) −*x*+1, −*y*+2, −*z*+1; (ix) −*x*+2, −*y*+2, −*z*+1; (x) −*x*, −*y*+1, −*z*.

Hydrogen-bond geometry (Å, º)

D—H···*A*	*D*—H	H···*A*	*D*···*A*	*D*—H···*A*
C15—H15···F1^{ii}	0.98 (2)	2.60 (2)	3.306 (2)	128.5 (17)

Symmetry code: (ii) −*x*−1, −*y*, −*z*.